Boundary conditions at a fluid – solid interface

Marek Cieplak[1,2], Joel Koplik[3] & Jayanth R. Banavar[2]
[1] *Institute of Physics, Polish Academy of Sciences, 02-668 Warsaw, Poland*
[2] *Department of Physics and Center for Materials Physics, 104 Davey Laboratory, The Pennsylvania State University, University Park, Pennsylvania 16802*
[3] *Benjamin Levich Institute and Department of Physics, City College of New York, NY 10031*

We study the boundary conditions at a fluid-solid interface using molecular dynamics simulations covering a broad range of fluid-solid interactions and fluid densities, and both simple and chain-molecule fluids. The slip length is shown to be independent of the type of flow, but rather is related to the fluid organization near the solid, as governed by the fluid-solid molecular interactions.

PACS numbers: 51.10.+y, 34.10.+x, 92.20.Bk

The principal theme of this paper is a study of the nature of the boundary conditions (BC) of fluid flow past a solid surface, a crucial ingredient in any continuum fluid mechanical calculation. The BC cannot be deduced from the continuum differential equations themselves, and it is often not easy to determine them experimentally. While the normal component of the fluid velocity must vanish at an impermeable wall for kinematic reasons, the parallel component, when extrapolated toward the wall, may match that of the wall only at some distance ζ away from it. This phenomenon is known as slip and ζ is the slip length [1]. Since the pioneering work of Maxwell [2], it has been recognized that the scale of ζ for a simple dilute gas is set by the mean free path λ of the fluid molecules, with an O(1) proportionality constant for a thermalizing wall. However, for a specularly reflecting wall, the proportionality constant could become large and lead to large slip. In the limit of low fluid density, ρ, λ becomes large suggesting that ζ would be large as well. Furthermore, in this limit the continuum approximation need not hold, and it is hard to glean the nature of the BC without a detailed knowledge of the influence of the fluid-solid interaction [3]. This is indeed the situation for micro-electro-mechanical systems [4] which operate in the Knudsen regime, in which λ can be larger than the system size. Earlier molecular dynamics (MD) studies have indicated substantial velocity slip for repulsive walls and deviations in hydrodynamic velocity profiles near the wall on lowering ρ [5–8].

In our MD simulations, we find that the flow profile in the middle of a channel does indeed correspond to that predicted by continuum theory, but we observe a range of behaviors near the walls. Our work provides a molecular basis for the large variability in the amount of slip observed experimentally [9]. We find that ζ is an excellent descriptor of the boundary conditions, independent of the channel width and the nature of the flow. Even at high densities, significant slip is induced on weakening the wall-fluid attraction. In the low ρ subcontinuum regime, a large ζ is found in virtually all cases, except for a chain molecule liquid and a strongly attractive wall. These two distinct classes of behavior lead to predictions amenable to experimental test. First, in a pressure driven flow, the speed with which fluid is transported shows a maximum as ρ is varied for all the large slip situations and none when the slip length remains small. Second, this maximum speed should scale linearly with the channel width for the large-slip case, but should scale quadratically (as in a dense fluid) for the small slip situation. Finally, our results indicate a strong link between the degree of slip at low ρ and the nature of fluid organization in the vicinity of the channel walls. In addition, we find analogous behavior in calculations of *thermal* slip, which arises when the two bounding walls of a channel are held at different temperatures [10].

In order to elucidate the BC as one lowers ρ from the dense liquid to the dilute gas regime, we consider a channel geometry and adopt the parametrization of Thompson and Robbins [6]. There are two parallel walls in the $x-y$ plane and N fluid atoms between the walls. Periodic BC are imposed along the x and y directions. In the monatomic case, two fluid atoms separated by a distance r interact with the Lennard-Jones potential $V_{LJ}(r) = 4\epsilon\left[(\frac{r}{\sigma})^{-12} - (\frac{r}{\sigma})^{-6}\right]$, where σ is the size of the repulsive core. As in Ref. [6], the potential is truncated at 2.2σ (and shifted). The MD studies are performed at a temperature $T = 1.1\epsilon/k_B$, which is just above the liquid-gas coexistence region for this model. The characteristic MD time unit $\tau_0 = \sqrt{m\sigma^2/\epsilon}$, where m is the atomic mass, is O(1 ps) for typical fluids. The walls are constructed from two [001] planes of an fcc lattice (96 atoms at each wall, with lattice constant 0.85σ), with wall atoms tethered to fixed lattice site by a harmonic spring with a large spring constant. For the narrowest channel studied here, the fluid atoms were confined to a volume $13.6\sigma \times 5.1\sigma$ in the $x-y$ plane and $L_0 = 12.75\sigma$

between the inner faces of the walls. The wall-fluid interactions are modelled by a distinct Lennard-Jones potential $V_{wf}(r) = 16\epsilon\left[(\frac{r}{\sigma})^{-12} - A\,(\frac{r}{\sigma})^{-6}\right]$. The parameter A determines the properties of the wall and varies between 1 and 0, corresponding to attractive and repulsive walls, respectively. Our earlier studies [11] of collisions between fluid molecules and this wall have quantitatively confirmed that A=1 corresponds to a purely thermal wall, and A=0 to a purely specular one.

The chain molecules comprising the polymeric fluid are composed of $n = 10$ Lennard-Jones atoms each. The consecutive atoms along the chain are tethered by the FENE potential [12], $V_{FENE} = -\kappa/2\, log[1-(r/r_0)^2]$, where $\kappa = 30\epsilon$ and $r_0 = 1.5\sigma$, which together with V_{LJ} keeps these atoms around $r = \sigma$ apart. This system is studied at $T = 1.6\epsilon/k_B$, which is above the liquid-vapor critical point, and the molecular diameter is small compared to the channel width (the radius of gyration of a molecule does not exceed 1.7σ). For either fluid, the equations of motion were integrated using a fifth-order predictor-corrector algorithm [13]. The spatial averaging was carried out in slabs of width $\sigma/4$ parallel to the z-axis. The high dilution data points were time averaged over 3 million τ_0 to reduce the noise. The results given here were obtained with a Langevin thermostat [13], but a Nose-Hoover thermostat [13] was found to yield virtually identical data. The T-dependent noise was applied in all directions during equilibration and only in the y-direction when data were collected. In the studies of thermal slip, the thermostat is applied only to the wall atoms, where we assign $T = 1.1\epsilon/k_B$ to one wall and $T = 1.3\epsilon/k_b$ to the other, and determine the variation of T across the channel.

The density profiles for the thermal slip simulation of the monatomic fluid are shown in Figure 1, for the attractive wall case (A=1). One can identify several layers near the wall, but at the center of the channel the profile becomes smooth. The value of density in the center, ρ, is used in the remaining plots as a measure of the fluid density. (A layered density profile is also characteristic of both monatomic and polymeric fluids without an imposed temperature gradient [11]). The density profile is asymmetric, as illustrated by the behavior of the density difference in the second layers between the cold and hot sides, $\Delta\rho_2 = \rho_{2c} - \rho_{2h}$, shown in the inset of Figure 1.

For both kinds of fluids, with and without a temperature gradient, the density in the first layer is largely ρ-independent, as shown in the top two panels of Figure 2 for the uniform-T case. There is, however, a noticeable difference in the behavior of the second layer. In the monatomic case, the density in the second layer undergoes a steady buildup from a negligible value, when ρ=$0.004\sigma^{-3}$ (corresponding to N=100, where 96 atoms coat the walls and the remaining 4 move essentially ballistically within the channel), to a saturation value when ρ becomes large. In the polymeric case, on the other hand, the second layer is almost fully constructed even at ρ=$0.002\sigma^{-3}$ and then its density varies only in a minor way. Thus the effective boundaries for the monatomic fluid undergo rapid transformation as a function of ρ, in contrast to the behavior of the chain molecule fluid.

The top and bottom panels of Figure 3 describe viscous and thermal slip, respectively, for the monatomic fluid. The velocity profile of the top panel was obtained for Couette flow. The central region has the expected hydrodynamic behavior – a linear velocity profile with constant shear stress for Couette flow, and a parabolic velocity profile with a linear shear for gravity-driven flow (not shown). While the temperature profiles in the thermal gradient case are remarkably similar to the velocity profiles in Couette flow, the dependence of the thermal slip length (defined analogously to the velocity slip length) on ρ is non-monotonic in a way that reflects the behavior of $\Delta\rho_2$. As seen in the middle panel of Figure 4 for A=1, the slip is a minimum at $\rho \approx 0.2\sigma^{-3}$, just where $\Delta\rho_2$ is maximal (see inset of Figure 1). Generally, the profiles predicted by continuum theory are seen either to persist to a point close to the wall (no slip), or else to terminate sooner, with a rapid change in profile around the second layer. It is the latter situation which is associated with slip, and it arises at very low ρ in most cases. Recently, Travis and Gubbins [14] have performed MD studies of velocity profiles for $A = \frac{1}{4}$ in gravity driven flows in a different parameter range: liquid densities, much narrower wall separation O(4σ), and with an acceleration an order of magnitude larger than used here. Presumably due to these differences, these authors obtained triple peaked velocity profiles with large contributions to the flow from the first layers.

The precise definition of the slip length ζ is given in terms of the position, z_0, at which the extrapolated fluid velocity reaches that of the wall (non-zero in the Couette case), as measured relative to the inner layer of the wall atoms. ζ is taken to be positive for z_0 outside of the channel and negative otherwise. Figure 4 summarizes our results on viscous and thermal ζ for monatomic and chain molecules. Viscous slip was studied in Couette and gravity driven flows and at various channel widths (two shown). We find a large variation in boundary conditions on changing the material parameters, in agreement with experimental observations [9]. However, the value of ζ is found to be *transferable* in that it neither depends on the kind of flow nor on the channel width. For a range of high ρ values for the monatomic fluid with wall interaction A=1, ζ is roughly equal to the negative of the distance between the wall and the second layer. At low

ρ, however, there is a rapid $\sim 1/\rho$ growth and a large slip.

The slip length is a sensitive function of the properties of the wall. When A=0, there is large slip even at high fluid densities, which is qualitatively consistent with the scenario of specular collisions with the wall. It is also reminiscent of the large slip found in MD studies of a nonwetting droplet on a solid surface [15] However, for intermediate values of A there is a complicated crossover behavior, as illustrated by the $\zeta - \rho$ curve for $A = \frac{1}{4}$ and $\frac{3}{8}$. In Ref. [8], a universal relationship between ζ and shear stress was found in the dense fluid regime on varying V_{wf}. Our large ρ data on ζ can similarly be collapsed by rescaling but our control of V_{wf} is through the parameter A as opposed to the amplitude of the full potential. The latter situation [8] would lead to a vanishing of the channel confinement in the zero amplitude limit.

The right-hand panel of Figure 4 shows that the variation of the viscous slip length ζ with ρ for chain molecules is more sensitive to A than for monatomic fluids. For $A = 1$, ζ becomes most negative as ρ tends to zero, while for $A = \frac{1}{4}$, ζ is large and positive even at high ρ (20.6σ for $\rho = 0.79\sigma^{-3}$). This result is qualitatively consistent with the MD results [16] on hexadecane in the vicinity of a solid surface, and with experiments on thin polymeric film drainage [17].

For monatomic fluids, the fluid velocity in the middle of the channel in a gravity driven flow exhibits a maximum as a function of ρ [11]. In contrast, the bottom panel of Figure 2 shows that, for chain molecules and A=1, the dependence of v_{max} on ρ is monotonic even though the viscosity at low ρ is substantially similar for the $n = 1$ and $n = 10$ fluids (data not shown). The large ρ behavior of v_{max} is dictated by the viscous effects associated with a dense fluid. The increase in v_{max} with ρ at low ρ for the monatomic case originates in the active reconstruction of the second layer. In contrast, for the chain molecule fluid, the organization near the walls remains largely unchanged (the chain molecules of the first two layers are stuck to the wall) so that viscous effects dominate the behavior of v_{max} even at small densities.

In summary, the two modes of behavior of ζ as ρ decreases to a small value, rapid growth or approach to a constant, are seen to be associated with distinctly different dependences of v_{max} on ρ. They also appear to be linked to the presence or absence of a density buildup in the second layer. Strikingly, the apparent complexity and non-universality of the BC is due to the microscale fluid physics in the vicinity of the solid interface.

This work was supported by KBN (Grant No. 2P03B-146-18), NASA, an NSF MRSEC grant, and the Petroleum Research Fund administered by the American Chemical Society.

[1] E. H. Kennard, *Kinetic Theory of Gases*, (McGraw-Hill, New York, 1938).
[2] J. C. Maxwell, *Phil. Trans. R. Soc. London.* Ser. A **170**, 231 (1867).
[3] Y. Sone, Annu. Rev. Fluid. Mech. **32**, 779 (2000).
[4] See, e.g., C.-M. Ho and Y.-C. Tai, Annu. Rev. Fluid. Mech. **30**, 579 (1998); D. C. Wadsworth, Phys. Fluids A - Fluid Dynamics, **5**, 1831 (1993); A. Beskok, G. E. Karniadakis, and W. Trimmer, J. Fluids Eng. - Trans. ASME, **118**, 448 (1996).
[5] J. Koplik, J. R. Banavar, and J. Willemsen, Phys. Fluids A **1**, 781 (1989).
[6] P. A. Thompson and M. O. Robbins, Phys. Rev. A **41**, 6830 (1990).
[7] M. Sun and C. Ebner, Phys. Rev. Lett. **69**, 3491 (1992).
[8] P. A. Thompson and S. M. Troian, Nature **389**, 360 (1997).
[9] See e.g. R. G. Lord in *Rarefied Gas Dynamics*, ed. J. L. Potter, AIAA, New York (1977), p. 531; F. M. Devienne, ed., *Rarefied Gas Dynamics*, Pergamon Press, New York (1960); S. A. Schaaf in *Modern Developments in Gas Dynamics*, ed. W. H. T. Loh, Plenum Press, New York (1969).
[10] A. Tenenbaum, G. Ciccotti, and R. Gallico, Phys. Rev. A **25**, 2778 (1982).
[11] M. Cieplak, J. Koplik, and J. R. Banavar, Physica A **274**, 281 (1999); and *ibid.* in press (cond-mat/0007132).
[12] M. Kroeger, W. Loose, S. Hess, J. Rheol. **37**, 1057 (1993).
[13] See, e.g. M. P. Allen and D. J. Tildesley, *Computer Simulation of Liquids* (Clarendon, Oxford, 1987).
[14] K. P. Travis and K. E. Gubbins, J. Chem. Phys. **112**, 1984 (2000).
[15] J. L. Barrat and L. Bocquet, Phys. Rev. Lett. **82**, 4671 (1999).
[16] M. J. Stevens, M. Mondello, G. S. Grest, S. T. Cui, H. D. Cochran, and P. T. Cummings, J. Chem. Phys. **106**, 7303 (1997).
[17] R. G. Horn, O. I. Vinogradova, M. E. Mackay, and N. Phan-Thien, J. Chem. Phys. **112**, 6424 (2000).

Figure captions

FIG. 1 Density profiles for the monatomic fluid undergoing thermal slip for walls with A=1. The tethering centers of the molecules comprising the inner wall are at the edges of the figure, and the values of density at the center of the channel, ρ, are indicated next to the histograms. The peak which is the closest to the wall denotes the first layer, and the second corresponds to the second maximum plus the elevated bin next to it. The inset shows the difference in the densities of the second layers in the vicinities of the cold and hot walls (the subscripts $2c$ and $2h$, respectively) as a function of the central density.

FIG. 2. The top two panels show the density, $\rho_i\sigma^3$, in the first (i=1, square symbols) and second ($i = 2$, circular symbols) layers for the indicated values of A. The top and middle panels are for the simple and polymeric fluids, respectively. The bottom panel shows the velocity of the polymeric fluid in the center of the channel vs. ρ, in gravity driven flow with $g = 0.01\epsilon/m\sigma$. L_0 refers to a channel of standard size and $2L_0$ corresponds to channels with twice the width. In all cases, the statistical errors are negligible.

FIG. 3. **Top:** Velocity profiles in Couette flow for various ρ, in the narrowest channel with attractive walls; the upper and lower walls move with velocities $\pm 0.1\sigma/\tau_0$, respectively. The slip length for the high ρ case is -1.7σ. **Bottom:** The temperature profile in the thermal slip problem. The open and closed circles correspond to ρ=0.773 and 0.004 σ^{-3} respectively. For ρ=0.193σ^{-3}, only the central slope is indicated.

FIG. 4. ζ (measured in units of σ) vs. ρ for viscous and thermal slip phenomena, for various values of A. The horizontal lines labeled I and II indicate the locations of the first and second layers, respectively. In all panels, triangles correspond to a channel of doubled width, and the remaining symbols are for the standard width. In the left and right panels, the solid and open symbols correspond to ζ, as determined from Couette and gravity driven (acceleration $0.01\epsilon/m\sigma$), flows respectively.

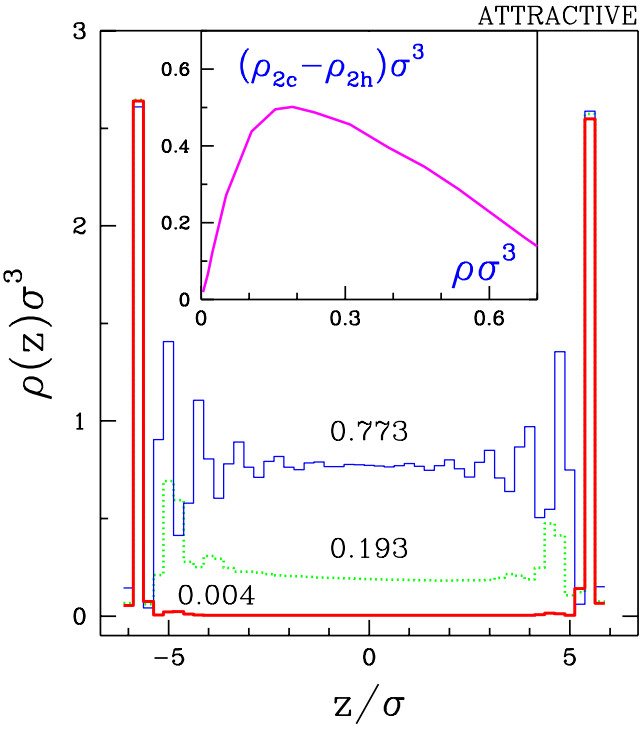

FIG. 1.

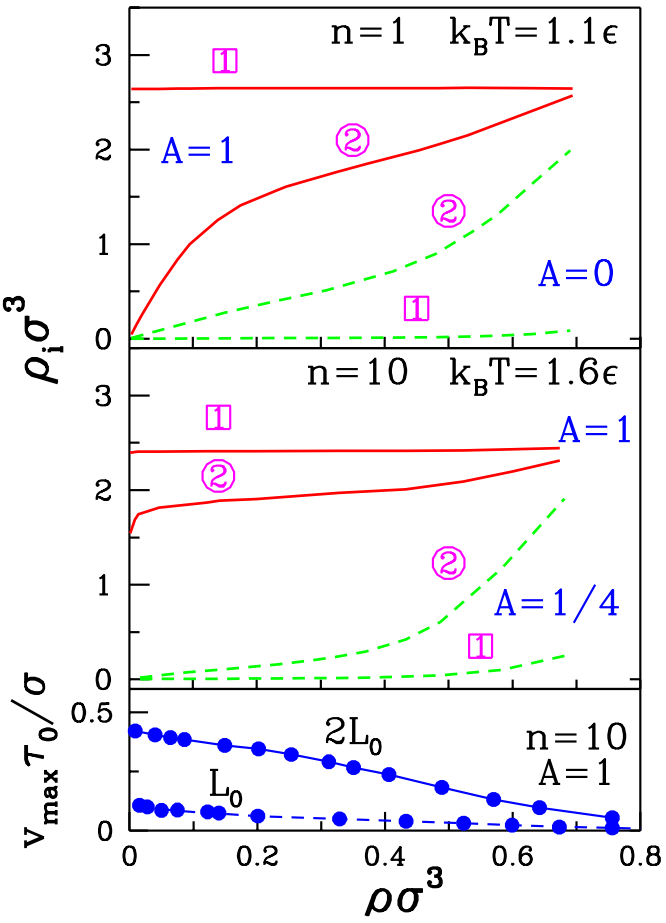

FIG. 2.

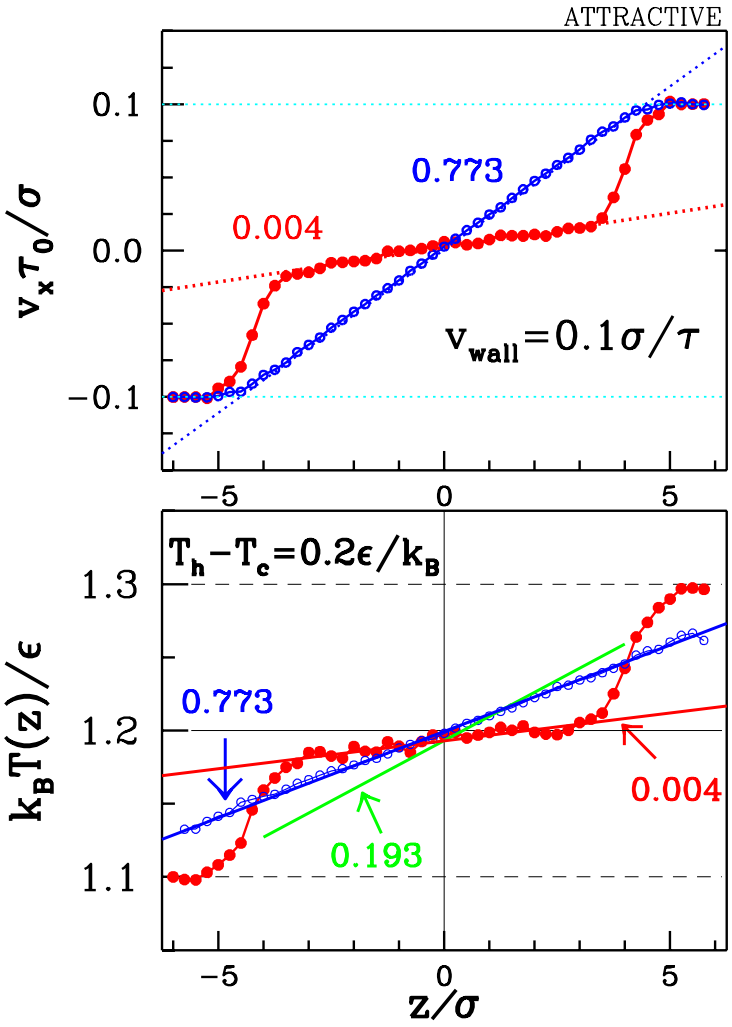

FIG. 3.

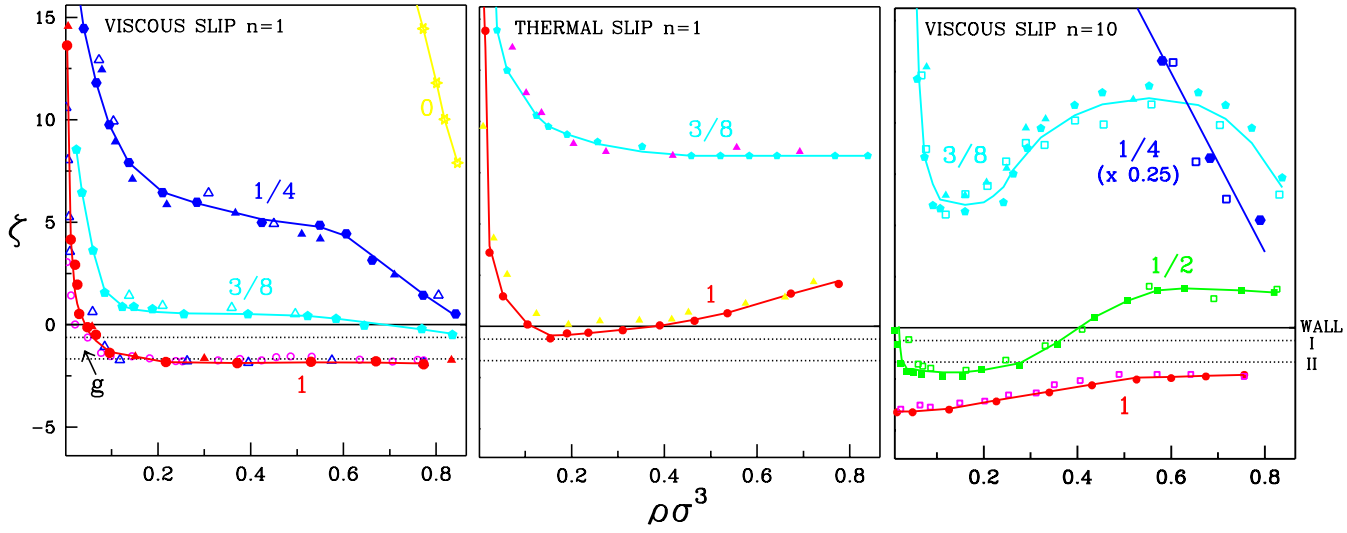
VISCOUS SLIP n=1
THERMAL SLIP n=1
VISCOUS SLIP n=10
ζ
ρσ3
0
1/4
3/8
1
g
1/2
(x 0.25)
WALL
I
II
15
10
5
0
−5
0.2
0.4
0.6
0.8

FIG. 4.